Journal of Soils and Sediments (2026) 26:43
https://doi.org/10.1007/s11368-025-04192-7

25TH ANNIVERSARY SPECIAL ISSUE - IMPACTS OF WILDFIRES ON SOIL AND SEDIMENT SYSTEMS

Suspended-sediment and phosphorus response in a fire-affected central Montana headwater catchment

Gregory D. Clark[1] · Michael W. Suplee[2] · Haylie M. Brown[1] · Molly A. Moloney[1] · Rodney R. Caldwell[1]

Received: 16 July 2025 / Accepted: 24 December 2025 / Published online: 11 February 2026

Abstract

Purpose Eutrophication and nuisance filamentous algal blooms (i.e. *Cladophora*) are increasingly common occurrences throughout much of the western United States. Wildfire may be contributing to the frequency and magnitude of algal blooms through excess sediment and nutrient loading to streams and rivers. Our objective was to evaluate the effects the 2021 Woods Creek Fire had on sediment yields and phosphorus (total and bioavailable) partitioning in Camas Creek, a major tributary to the Smith River in Montana where *Cladophora* are now consistently reaching nuisance levels.

Methods We collected water quality samples during snowmelt pulsing events as well as fixed interval sampling using an established U.S. Geological Survey stream gage instrumented with a continuous water quality sonde and an automatic peristaltic pump sampler. Water samples were processed for total phosphorus (TP), sediment-bound bioavailable phosphorus (S-BioP), soluble reactive phosphorus (SRP), and suspended sediment concentrations and were evaluated using linear regression and other nonparametric statistical tests. Continuous turbidity and streamflow were evaluated using hysteresis analysis to determine sediment sourcing and connectivity.

Results We found that the Woods Creek Fire did not significantly influence TP and S-BioP in Camas Creek. However, there was a significant increase in SRP and turbidity in both postfire years (2022 and 2023). Hysteresis analysis of 91 delineated events indicated positive (clockwise) hysteresis was the dominant event pattern during the snowmelt period. This may indicate a lower hillslope to channel connectivity, with the major sediment supply originating from the channel and/or riparian areas.

Conclusion Results from this study demonstrate the benefits of combining discrete water quality samples with high-frequency turbidity sensors to characterize postfire sediment and phosphorus dynamics. While a lack of postfire response in TP and S-BioP is contrary to many other studies, our findings highlight the role climate and catchment morphology play in attenuating a disturbance effect.

Keywords Wildfire · Sediment · Turbidity · Phosphorus · Snowmelt

1 Introduction

Excessive growth of filamentous algae and eutrophication is a common occurrence in rivers throughout much of the western United States (U.S.). Problems associated with nuisance filamentous algal blooms include but are not limited to clogging of streambed material and irrigation pumps, excessive diurnal swings in dissolved oxygen (Stevenson et al. 2012), aesthetic impairment (Suplee et al. 2009; Jakus et al. 2017), and accumulation of harmful levels of *Escherichia coli* (Wurtsbaugh et al. 2019). *Cladophora* is one of the most widespread forms of green filamentous algae that naturally grows on stable hard substrates where temperature, light, and nutrients are conducive to growth (Dodds 1991),

Responsible editor: Kristen Kieta

✉ Gregory D. Clark
gdclark@usgs.gov

[1] Wyoming-Montana Water Science Center, U.S. Geological Survey, Helena, MT, USA

[2] Montana Department of Environmental Quality, Helena, MT, USA

and can rapidly grow to nuisance proportions under certain conditions. Nuisance levels of *Cladophora* are driven by a range of interacting natural and anthropogenic factors. The key factors for *Cladophora* growth are sufficient nutrients (i.e., nitrogen and phosphorus), a suitable water temperature range, and streamflow (Dodds et al. 1997; Vadeboncoeur et al. 2021). These factors are highly susceptible to shifts in climate and landscape characteristics. For example, landscape-scale disturbances such as resource extraction, urbanization, agriculture, and wildfire can greatly affect each element contributing to eutrophication of surface waters in the western United States (Withers et al. 2014; Watt et al. 2021; Zhou et al. 2022).

Wildfires are a natural and ubiquitous disturbance in many ecosystems that can drastically change landscape characteristics and watershed function. The magnitude of wildfire disturbance is often described and measured in terms of burn severity which is influenced by fire duration, fuel loading, topography, and weather at the time of the fire. While low severity fires often promote resilience and biodiversity (Burkle et al. 2015; Strand et al. 2019; Koontz et al. 2020), moderate to high severity fires can result in profound changes to a watershed's structural configuration and sediment connectivity (Wester et al. 2014; Williams et al. 2016). Wildfires increase catchment availability of fine sediments consisting of clay, silt, and ash that serve as the primary vector for phosphorus transport (Malmon et al. 2007; Withers and Jarvie 2008; Jumps et al. 2022; Neely et al. 2024). Shortly after a fire, fine-grained ash particles can be transported and deposited by surface runoff in valley depressions or footslopes (Bodí et al. 2014; Follmi et al. 2022) and directly to a river or stream, resulting in ash- and charcoal-rich discharges (Ryan et al. 2011). While the flux of ash and charcoal may be short-lived, the material deposited in flood plains and alluvial fans can be sequentially remobilized during precipitation and snowmelt events (Murphy et al. 2019; McGuire et al. 2024). Wildfires also serve as a weathering agent through thermal degradation of soil particles. When soil is exposed to extreme temperatures, the organic binding agents and clay aggregates begin to degrade (Neary et al. 2005), decreasing aggregate stability and creating finer particles that are more susceptible to erosional processes (Mataix-Solera et al. 2011). Deposition of fine sediment in the river channel can lead to substantial longitudinal geomorphic changes within a river system (Shakesby and Doerr 2006; Rengers et al. 2021; Busby and Wilcox 2024) and deposition of fine sediment in municipal water supply reservoirs may degrade water quality and reduce water storage capacity (Smith et al. 2011; Bladon et al. 2014; Hohner et al. 2019; Robinne et al. 2021; Stone et al. 2021). Sediments supply nutrients, such as phosphorus, and organic compounds necessary for terrestrial and aquatic life, but the overabundance of suspended sediment can also lead to the impairment of freshwater ecosystems. Silt and clay amount to a small fraction of the total sediment load transported in fluvial systems but can contribute a substantial load of adsorbed contaminants due to their high surface areas and mineralogy (Owens et al. 2005).

Because wildfires increase sediment loads, it is also observed that they can increase the concentration of phosphorus in receiving waters. Large surface areas and the presence of iron and aluminum oxyhydroxides on fine sediment enables it to serve as the main vector for phosphorus transport and labile phosphorus in fluvial systems under typical pH ranges (5–8) (Temporetti et al. 2019; McDowell and Sharpley 2003). Phosphorous within sediments and ash are susceptible to both desorption and physical erosion processes, increasing the potential for export of phosphorus in both dissolved and particulate form (Lane et al. 2008; Schaller et al. 2015). Sediment that can bind phosphorus comprises both organic and inorganic particulate forms, but the inorganic fraction contains the bulk of phosphorus that can be released into the water. Release of phosphorus from sediment particles can occur by desorption at alkaline pH values, as a result of equilibrium reactions when water concentrations of soluble phosphorus become very low, due to displacement by competing ions such as sulphate, or by dissolution of Fe- and Al- oxyhydroxides (Froelich 1988; Records et al. 2016). Once mobilized, phosphorus then becomes available for biotic uptake as orthophosphate, which is typically quantified as soluble reactive phosphorus (SRP).

Wildfire-associated excess phosphorus has been observed at a range of temporal scales. Hauer and Spencer (1998) report excessive amounts of phosphorus lasting 3–5 years after the fires while Yu et al. (2019) find elevated SRP concentrations lasting up to 10 years post-fire. In some cases, there may be legacy effects of sediment and sediment-bound phosphorus from high severity fire in watersheds with low sediment connectivity (Emelko et al. 2016; Wilkes et al. 2019). The buffering capacity of riverbed sediments may be reduced in fluvial systems that have higher ambient levels of particulate phosphorus causing an excess amount of bioavailable phosphorous in solution and promoting the production of algal biomass (Records et al. 2016).

Our objective was to evaluate the effects the 2021 Woods Creek Fire had on sediment yields and phosphorus (total and bioavailable) partitioning in Camas Creek, a major tributary to the Smith River in Montana. The Smith River is a significant economic, agricultural, and recreational resource receiving well over 4,000 visitors a year (Freistadt et al. 2024) and has recently experienced an increase in *Cladophora* bloom occurrence resulting from increased water temperatures and lower flows (Bell et al. 2024), making it particularly beneficial to understand the potential impact wildfires might add to an already stressed river. We used a combination of discrete sampling and continuous water-quality monitors to examine the response in suspended-sediment and phosphorus concentrations for a 2-year period following the fire (water years 2022 and 2023; water year defined as the period between October 1 and September 30 of the following year and named for the calendar year in which it ends). We then compared the results to those collected one year before the fire (water year 2020). Results can further inform watershed managers on the impacts wildfires may have on sediment and phosphorus concentrations and may be transferable to other thermally stressed, nutrient rich rivers in the region.

2 Data and methods

2.1 Site description

Camas Creek drains the eastern side of the Big Belt Mountains, an island range east of the continental divide in central Montana. U. S. Geological Survey (USGS) streamflow gaging stations were operated at or near the confluence of Camas Creek and the Smith River in 2020 (USGS 06076600) and 2021–2023 (USGS 06076590). The watershed upstream from the monitored location drains approximately 154 km^2 of forest and rangeland ranging in elevation from 1411 m to 2724 m with a mean slope of 21.9% (U.S. Geological Survey, 2019). Soils are primarily composed of well drained cryepts and ustolls (Natural Resources Conservation Service 2024, 2025) overlying fine grained sedimentary rock in the Belt Supergroup (Reynolds and Brandt 2005). Landcover in the watershed is evenly split between rangeland in the lower elevations and forest in the higher elevations. Forests are primarily composed of *Pseudotsuga menziesii* and *Pinus contorta* (Riley et al., 2021). Climate is characterized by long cold winters and short warm summers. Mean annual precipitation is approximately 668 mm, most of which occurs as snow from October through April (U.S. Geological Survey 2019). Its hydrologic regime is snowmelt dominated with the highest flows occurring in late May through June.

A lightning strike on July 10, 2021, ignited the Woods Creek Fire in the Big Belt Mountains of central Montana, burning approximately 22,662 hectares before its containment. Damage to the soils was estimated at 40% low and 33% moderate to high soil burn severity, with the remaining 27% as unburned (Burn Severity Portal 2021). Areas of moderate to high soil burn severity were primarily confined to the densely vegetated north-facing headwaters of Big Birch Creek and Camas Creek. Both Big Birch Creek and Camas Creek are major tributaries to the Smith River.

2.2 Sample collection and data analysis

2.2.1 Climate, Precipitation, and streamflow

Discharge was collected from USGS-06076600 (46.70431, −111.19278) before the fire in 2020, and from USGS-06076590 (46.67824, −111.19388) after the fire in 2022 and 2023. Discharge data for both locations is retrievable from the National Water Information System (U.S. Geological Survey 2025). Due to access issues after 2020, the monitoring location was moved from USGS-06076600 to USGS-06076590 which is approximately 3.4 km further upstream on Camas Creek (Fig. 1; comparability of the two sites will be discussed below, in Sect. 2.2.6). Discharge was measured from gage height using methods described in Turnipseed and Sauer (2010). A 20-year median daily discharge was estimated from a long-term USGS gage (USGS-06076690) downstream from the Camas Creek stream gage using a maintenance of variance extension performed with the smwrStats package in R (R Core Team 2024). Precipitation data was retrieved from the Natural Resource Conservation Service Snow Telemetry (SNOTEL) network at Pickfoot Creek (Station 690; U.S. Department of Agriculture, 2025). Station 690 is within the Camas Creek watershed at an elevation of about 2,036 m.

2.2.2 Continuous water quality and discrete sample collection

Water-quality sampling was conducted at USGS-06076600 in 2020 as part of a collaborative effort between the USGS and the Montana Department of Environmental Quality (MDEQ) to identify nitrogen and phosphorus contributions to the Smith River. This collaboration continued after the Woods Creek Fire, when water-quality was collected at USGS-06076590 in 2022 and 2023 to quantify the effects of the fire. At both sites, turbidity was measured in formazin nephelometric units (FNU) at 15-minute increments following protocols outlined in Wagner et al. (2006) using a YSI EXO turbidity probe (YSI, Yellow Springs, OH). Samples were collected at routine intervals approximately 2 weeks apart as well as during high turbidity events using an automated sampler (ISCO 3700, Teledyne ISCO, Lincoln, NE) when turbidity exceeded a threshold based on ambient stream conditions. When an event occurred and the automatic sampler triggered, three 450 ml bottles were filled sequentially and considered as one sample. The automatic sampler

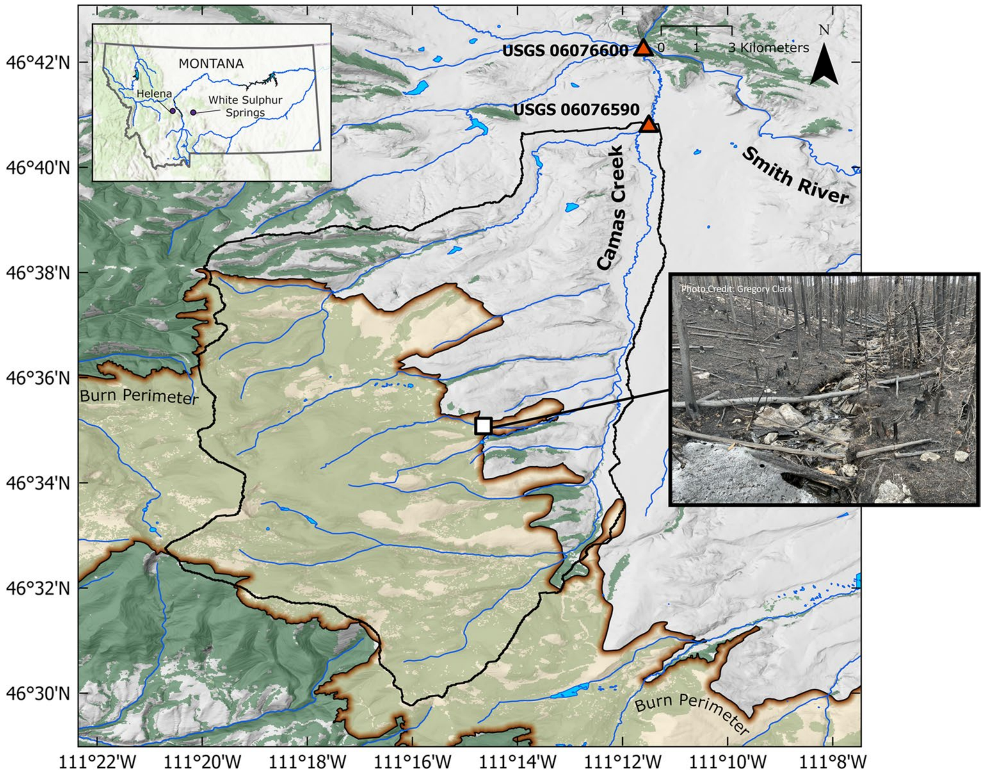

Fig. 1 Study area map with insert photograph showing Mule Creek (tributary to Camas Creek) after the 2021 Woods Creek Fire. Green shading indicates forested, and grey indicates unforested as determined using the National Land Cover Database (Geological Survey 2024). Camas Creek watershed boundary is shown with a thick black line and monitored locations are orange triangles labeled with their respective USGS stream gage number (U.S. Geological Survey 2025). Woods Creek Fire perimeter is overlayed as a shaded region. Burn area is from Monitoring Trends in Burn Severity (2022)

then collected a sample every hour turbidity exceeded the turbidity threshold until all bottles ($n = 24$) were filled or turbidity fell below the trigger threshold. Data presented herein are a combination of fixed-interval and targeted turbidity-triggered event samples.

2.2.3 Suspended sediment and phosphorus (Total, bioavailable, soluble)

The three bottles were then separated for processing. One bottle was reserved unfiltered for total phosphorus (TP), one was filtered through a 0.45 µm disk filter for soluble reactive phosphorus (SRP), and one was for suspended-sediment concentration as both total suspended solids (TSS; Standard Methods 2017) and suspended-sediment concentration (SSC; Guy 1969). TSS is typically measured by passing an aliquot of sample through a filter and measuring the dry weight of the residue whereas SSC measures the dry weight of all sediment in the sample and more accurately accounts for larger particles (Gray et al. 2000). Though SSC is a more accurate method, TSS is widely used by State environmental agencies and available in public data portals such as the Water Quality Poral (National Water Quality Monitoring Council 2025). TP and SRP samples were placed on dry-ice and kept frozen prior to laboratory analysis. Periodically, bottles were designated to determine the amount of sediment-bound bioavailable P (S-BioP) per the analytical method in Suplee (2021). S-BioP samples were processed in batches, with each batch having an associated deionized (DI) water blank. For each batch, the DI water blank's S-BioP concentration (if above zero) was subtracted from each associated S-BioP sample result. In a few cases, contamination in the DI water blank exceeded the analytical result for a sample, resulting in a negative value. Resulting blank-adjusted values less than zero were replaced with zero for purposes of carrying out analyses herein. Although discharge was available, we did not compute a flux and chose to focus our analyses on concentration of the various phosphorus forms and the linkage it may have with turbidity and suspended sediment.

For the purposes of this study, we focused on determining whether sediment transported during runoff originated from upland areas (distal) or from resuspension of sediments within the channel (proximal). To do so, we analyzed event hysteresis using turbidity as a proxy for suspended sediment. Hysteresis occurs when the magnitude of turbidity for any given value of streamflow differs on the rising limb of the hydrograph from the same value of streamflow on the falling limb. We used an index-based approach outlined by Lloyd et al. (2016) to characterize the event and catchment transport behavior. The index is calculated by averaging the difference in turbidity measured on the rising and falling limbs of streamflow. We chose to average at 5% increments of streamflow from an events minimum flow to its maximum.

2.2.4 Comparison of the pre- and postfire sampling locations

The similarity of the downstream prefire site (USGS-06076600) to the upstream postfire site (USGS-06076590) was evaluated to be confident that any water quality changes observed were the result of fire effects and not a spurious treatment effect due to the site move. One prefire dataset and one postfire dataset were available for this purpose. Prefire, TSS and TP data were available from 2020 at USGS-06076600, and equivalent data were also collected prefire in spring and early summer 2021 at the upstream site (USGS-06076590). TP was regressed against TSS for each monitored location, and these regressions were compared using analysis of covariance (ANCOVA). Postfire, a one-day synoptic sampling of water quality was undertaken at two sites in July 2022. USGS-06076590 was sampled along with a new site nearer to the mouth. Since USGS-06076600 could no longer be accessed, sampling occurred as close to it as possible and downstream from a center-pivot irrigation project on the creek's west side.

2.2.5 Statistical analysis and data availability

Analyses were carried out in R (R Core Team 2024). Continuous turbidity was compared across the three study years using pairwise Kolmogorov-Smirnov tests based on the kernel density estimates. Pre- and postfire SSC in mg L^{-1} was compared using simple linear regression, with turbidity as the explanatory variable and measured SSC as the dependent variable. Phosphorus is closely associated with suspended sediment in flowing waters and TP concentrations are often tightly correlated with TSS concentrations or surrogates like turbidity (Froelich 1988; Grayson et al. 1996; Uusitalo et al. 2000). Therefore, we compared linear regressions of phosphorus concentrations as TP, SRP, and BioP (e.g., turbidity vs. TP) between three time periods (prefire year 2020, postfire year 2022, and postfire year 2023) using ANCOVA with a significance threshold p-value of 0.05. For cases where a significant difference was found between the regression lines, pairwise comparison was then applied using estimated marginal means with a Bonferonni adjustment to identify grouping patterns (Searle et al. 1980). Box and whisker plots of phosphorus form concentrations for the three spring-to-early summer runoff periods are also presented.

3 Results

3.1 Comparability of the pre- and postfire sampling sites

There was no evidence that moving from the downstream site at USGS 06076600 to the upstream site at USGS 06076590 induced an effect resulting in a significant change in the TSS-TP relationship. There was no significant difference (ANCOVA; $p=0.230$) between the two site's regression lines (Fig. 2A). However, the regression for the downstream site is strongly affected by a single high TSS point; if this point is removed and the data regressed again, ANCOVA still indicates that there is no significant difference between the two lines ($p=0.260$; Fig. 2B).

Data from the 2022 postfire synoptic sampling (Table 1) have very similar TSS: TP ratios for both sites (0.0039 at USGS-06076600 and 0.0032 at USGS-06076590). Slopes from the prefire (2020 and 2021) TSS versus TP regressions in Fig. 2A were also very similar (0.0014 at USGS-06076600 and 0.0017 at USGS-06076590). Further, the two sampling sites showed nearly identical specific conductivity and SRP. The pH value was higher downstream, but pH usually increases steadily towards midday in moderately productive streams (Nimick et al. 2011) and the downstream site was sampled later in the day. The downstream temperature increase is also likely due to the later time of day.

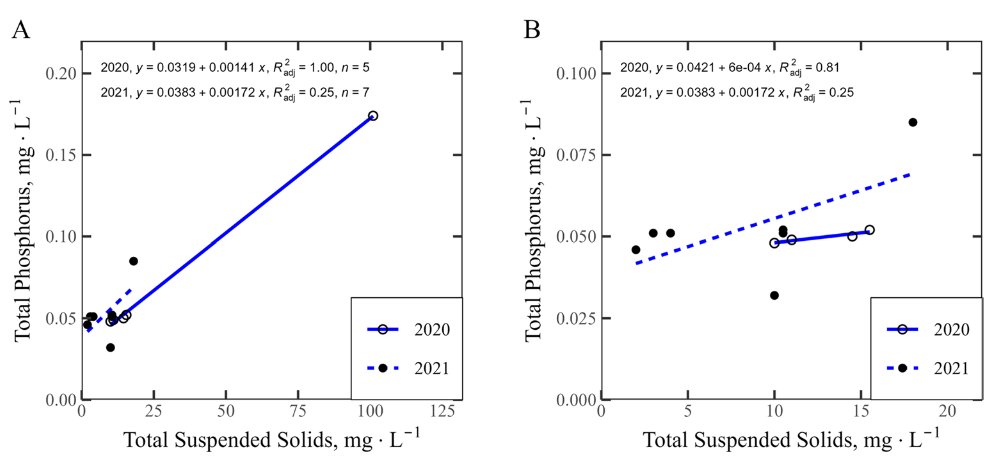

Fig. 2 Regression plots showing the relationship between total phosphorus (TP) and total suspended solids (TSS) both with single outlier (**A**) and without (**B**)

Table 1 Results for postfire synoptic water quality sampling on Camas creek

Location	Latitude	Longitude	Date & Time	Water Quality Parameter					
				Water Temp. (°C)	pH	Specific Conductance (μS cm^{-1})	TSS (mg L^{-1})	TP (mg L^{-1})	SRP (mg L^{-1})
USGS-06076590	46.678	−111.194	7/16/2022 10:41	13.8	7.86	330.9	14	0.055	0.027
USGS-06076600	46.662	−111.188	7/16/2022 11:39	16.2	8.28	331.9	20	0.065	0.028

Overall, there is sufficient evidence indicating that the move to the upstream site at USGS-06076590 did not introduce a significant treatment effect, and therefore any changes observed at USGS-06076590 can reasonably be attributed to the fire and not to the site move.

3.2 Streamflow and hydroclimatic conditions

Interannual streamflow conditions differed substantially during the study years. Streamflow in central Montana is controlled by seasonal snowpacks, with average annual streamflow reaching a maximum in late May or early June (Fig. 3). The 20-year median peak flow estimated from USGS-06076690 (refer to methods) was 2.1 $m^3 s^{-1}$ typically occurring on June 03. Streamflow was above the estimated 20-yr median in 2020 with a peak flow of 3.8 $m^3 s^{-1}$ occurring on June 2, 2020. After the fire, the two study years were markedly different in terms of streamflow and snowpack. Postfire year 1 (2022) was considerably drier with a peak of 0.733 $m^3 s^{-1}$ on June 21, below the estimated median streamflow. Streamflow in postfire year 2 (2023) was well above the estimated median with a peak flow of 6.1 $m^3 s^{-1}$ occurring approximately one month earlier on May 5, 2023. Streamflow in 2023 remained above the estimated median for much of the year.

Observed streamflow corresponded well with snow water equivalent (SWE) recorded at the Pickfoot snow telemetry station (SNOTEL 690, Fig. 4) located within the Camas Creek watershed. Water year (WY) 2022 was a historically low snowpack year with a peak SWE of 61 mm occurring on April 24. WY 2023 was near normal, with a peak SWE of 251 mm occurring on April 23. The long-term median peak SWE is 277 mm occurring on April 2.

3.3 Phosphorus (total, bioavailable, soluble)

The turbidity versus TP relationship for the three time periods is shown in Fig. 5A. Per ANCOVA, there was a significant relationship between turbidity and TP ($p<0.001$), but no significant difference in the turbidity versus TP relationship between any of the three time periods ($p=0.499$). Linear regression correlation coefficients indicated a strong relationship in 2020 (adj-$R^2=0.87$) and 2023 (adj-$R^2=0.92$), but a weak relationship in 2022 (adj-$R^2=0.15$). In the boxplot (Fig. 5B), note the high degree of overlap in TP concentrations for the three time periods; each plot represents snowmelt influenced spring/early summer runoff.

Per ANCOVA, there is a significant relationship between turbidity and S-BioP ($p=0.001$; Fig. 5C), but no significant difference in the turbidity versus S-BioP relationship between any of the three time periods ($p=0.600$). In the boxplot (Fig. 5D), there is a high degree of overlap in S-BioP concentrations for the three time periods; each plot represents snowmelt influenced spring/early summer runoff.

Per ANCOVA, there was a significant relationship between turbidity and SRP ($p<0.001$; Fig. 5E), and there was a significant difference between at least two of the years ($p=0.009$). Based on Tukey's Honest Significant Difference (HSD), prefire year 2020 had a significantly different relationship from postfire year 2023, and postfire year 2022 had a significantly different relationship from postfire year 2023. Figure 5F shows the boxplots for SRP for the three time periods; each plot represents snowmelt influenced spring/early summer runoff.

The relationship between TP and S-BioP is shown in Fig. 6. S-BioP is a sub-component of TP, and it is expected that the TP: S-BioP ratio will be ≤1. Per ANCOVA, there was a significant relationship between TP and S-BioP ($p<0.001$), but no significant difference between the TP vs. S-BioP relationship for any of the three time periods ($p=0.563$). Over the course of the study, pre- and post-fire, the overall relationship between TP and S-BioP is best explained as a curvilinear second order polynomial (Fig. 6) with an adjusted R^2 of 0.42.

3.4 Turbidity, suspended sediment, and hysteresis

Before the Woods Creek Fire, turbidity and suspended sediment pulses were driven by snowmelt. The highest turbidity value recorded during the prefire study period was 165 FNU at peak streamflow for the year and the highest suspended-sediment concentration was 185 mg L^{-1} sampled on May 20. In postfire year 2022, the maximum recorded turbidity was 601 FNU and occurred shortly after a convective storm on July 25, 2022, during which sediment concentrations were measured at 1330 mg L^{-1}. Despite the elevated snowpack and higher streamflow, turbidity was considerably less flashy in 2023 with a maximum turbidity of 167 FNU occurring after a storm on August 26, 2023, during

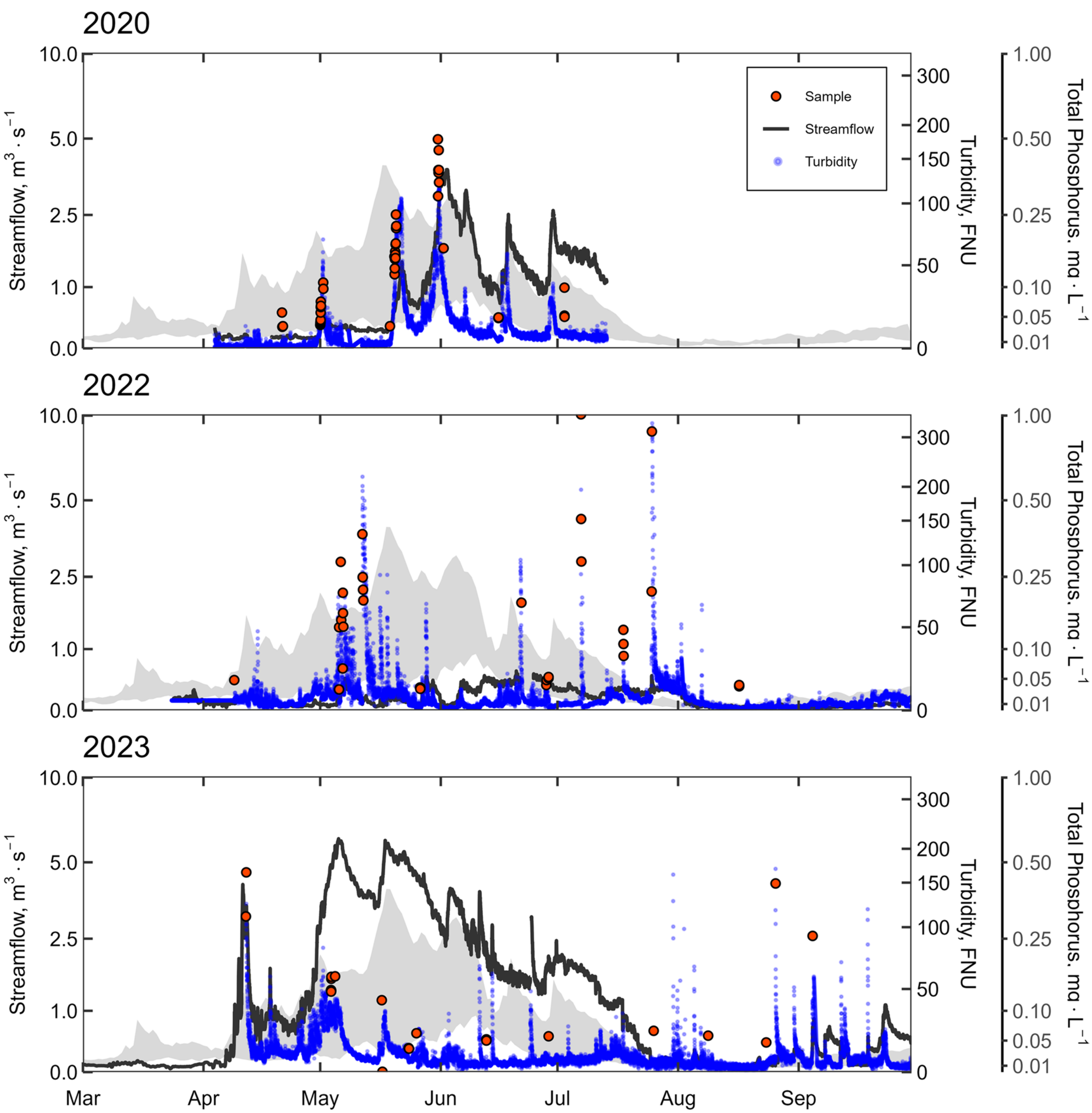

Fig. 3 Time-series plots showing prefire (2020) and postfire (2022 and 2023) 15-min turbidity in formazin nephelometric units (FNU) and streamflow in cubic meters per second as well as discrete sample results for total phosphorus (TP) in milligrams per liter. The shaded grey region is one standard deviation for the 20-year estimated mean daily streamflow

which sediment concentrations were measured at 346 mg L^{-1}. Although the highest turbidity recorded was during the postfire period, it was for a short period of time in response to intense rainfall instead of snowmelt.

Figure 7A (below) shows the relationship between turbidity and SSC for the three studied time periods. Postfire years 2022 and 2023 show a strong correlation between SSC and turbidity with an adjusted-R^2 of 0.95 and 0.82, respectively. The relationship during the prefire year showed a weaker correlation with an adjusted-R^2 of 0.67. Testing the regressions with ANCOVA indicates there is a strong significant relationship between turbidity and SSC for all study years and there is a significant difference between years (*p*-value < 0.001). A post-hoc Tukey's multiple comparison test revealed the significant difference was between prefire year 2020 and postfire year 2022 (p-value < 0.005).

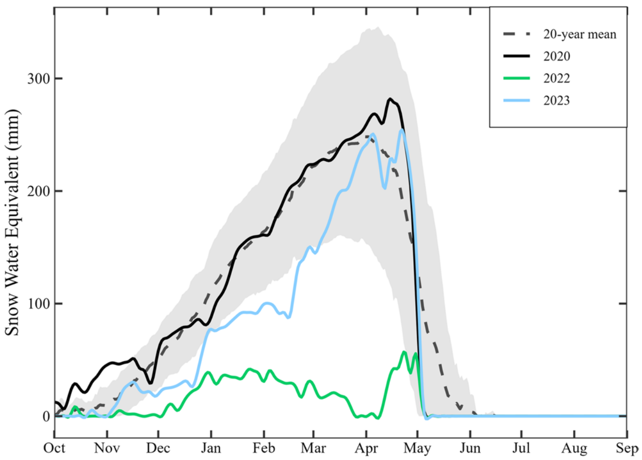

Fig. 4 Time-series plot showing daily snow water equivalent for the Pickfoot SNOTEL station (Station 690; U.S. Department of Agriculture 2025). Shaded grey region represents one standard deviation for the 20-year daily mean

In summary, prefire and postfire turbidity were comparable. In both prefire and postfire periods, turbidity exceeded 6 FNU approximately 50% of the time (Fig. 7B). Despite this, the postfire years had a higher baseline turbidity. We chose to define baseline turbidity as the magnitude of turbidity corresponding to the mode of the kernel density distribution. Baseline turbidity increased from 1.5 FNU in 2020 to 3.3 FNU in 2022 and 5.4 FNU in 2023 (data not shown). These baseline estimates correspond well with the 95% probability of exceedance estimates which were 0.6 FNU in 2020, 1.4 FNU in 2022, and 2.6 FNU in 2023 (Fig. 7B). A pairwise Kolmogorov-Smirnov test indicated that postfire turbidity was higher in both 2022 and 2023 (p-value $<$ 0.001), and that turbidity was higher in 2023 relative to 2022 (p-value $<$ 0.001).

3.5 Event hysteresis assessment of sediment connectivity and source contributions

We analyzed 91 events across all three monitored seasons. There were 14 events in 2020 with an average hysteresis index (HI) of 0.216 ± 0.063 (mean ± standard error), 38 events in 2022 with an average index of 0.150 ± 0.034, and 38 events in 2023 with an average index of 0.164 ± 0.039. There was little variation in event behavior seasonally (Fig. 8) with predominantly positive indices. Despite the overall positive hysteresis patterns, postfire year 2023 had the greatest variability (Fig. 8). Postfire years did exhibit more negative HI events with 13 in 2022 and 11 in 2023, though the majority of these occurred after snowmelt in July and August in response to convective precipitation.

The highest hysteresis index (HI = 0.618) during the study occurred on June 21, 2022, six hours before streamflow reached its annual peak. The lowest hysteresis index (HI = −0.275) during the study was recorded that same year after snowmelt concluded on July 25, 2022, when turbidity reached a maximum 1.5 hours after streamflow crested (Fig. 3).

4 Discussion

To our knowledge, this is the first study examining changes in stream sediment-bound bioavailable phosphorus (S-BioP) concentrations before and after a wildfire. The principal characteristics of the S-BioP we quantified are (a) it is only loosely adsorbed to the surface of suspended particles (inorganic and organic) and therefore can readily desorb into solution under the proper biogeochemical conditions, and (b) it is strongly correlated with bioavailable phosphorus quantified via algal bioassay methods (Hanna 1989; Uusitalo and Ekholm 2003). The current study shows that S-BioP and TP concentrations were not significantly altered by fire in this watershed, nor did fire alter the relationship observed between these two forms of P (Fig. 6). This result was unexpected, as a synthesis of fire effects on stream water quality globally (Ranalli 2004), in the western United States (Rust et al. 2018), and for a case study in Montana (Hauer and Spencer 1998) all show that fire can increase phosphorus concentrations downstream of fire-burned areas. In a Mediterranean woodland, Souza-Alonso et al. (2024) report that fire severity is the principal driver of fire effects on soil phosphorus, with low severity fires having little effect while moderate to severe fires having varying effects and complex recovery trajectories, depending on soil characteristics. Collectively, fire effects on TP and S-BioP concentrations in the current study were not statistically significant, however there is a general pattern across all three phosphorus forms. Specifically, phosphorus in runoff during the first spring after the fire (postfire year 2022), relative to turbidity, was lower than before the fire (Fig. 5A, C, E). Then, during spring runoff of the second year after (postfire year 2023) the fire, phosphorus concentrations (relative to turbidity) were higher than before the fire.

There is some evidence to suggest this lagged response in phosphorus may result from an increase in fine sediment loading after the fire. Turbidity was significantly higher in both postfire years, with the greatest difference in baseline turbidity. An increase in fine sediment loading may also help explain the slight differences in turbidity and SSC regressions between the three studied periods. Bright and Mager (2020) showed that among the properties affecting turbidity the most, fine particles and organic matter were among the most significant. Wildfires are known to increase fine sediment fractions with some studies reporting as much as a 50% increase in the proportion of silt and clay (Malmon et

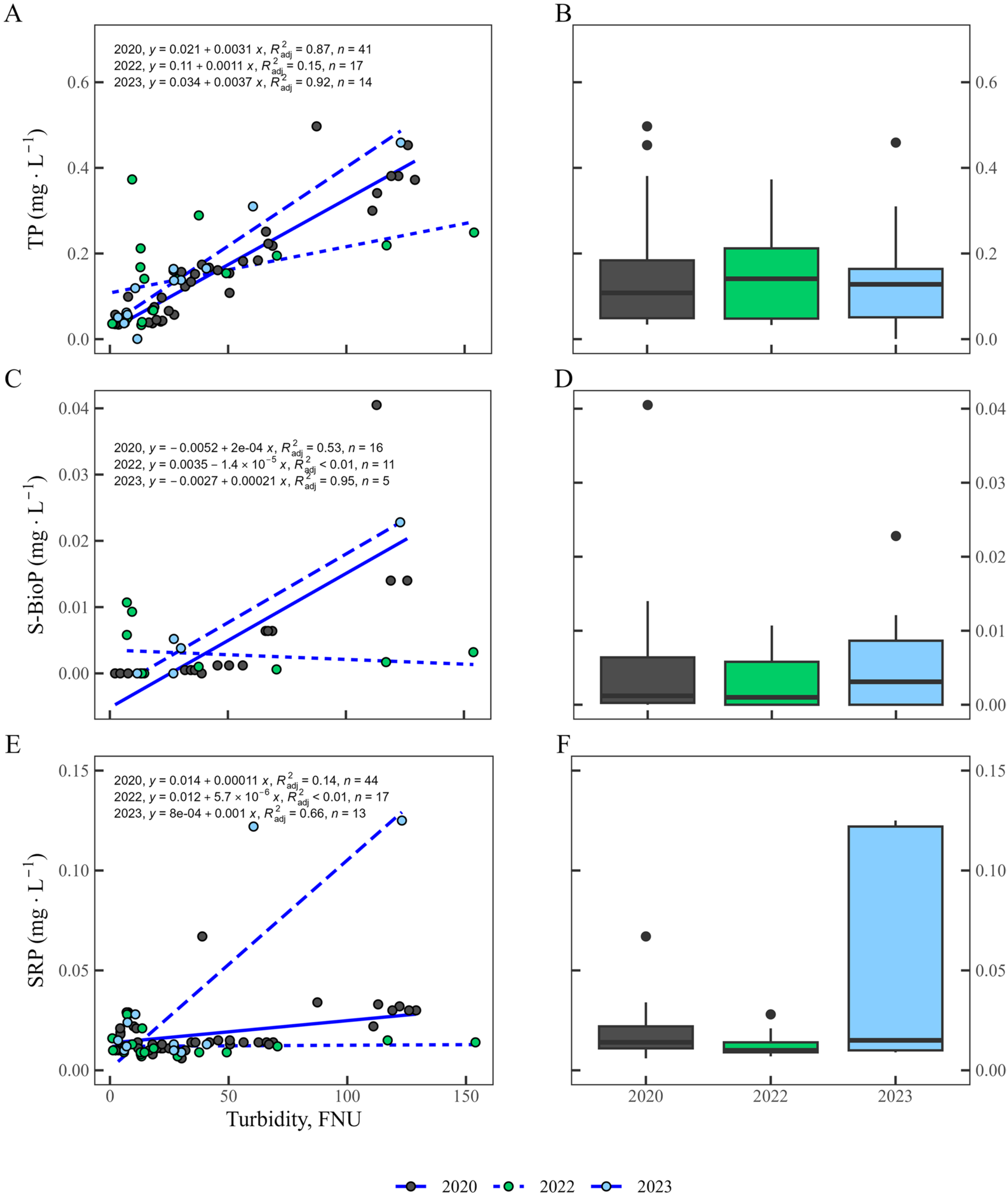

Fig. 5 (**A**) Regressions relating total phosphorus (TP), (**C**) sediment-bound bioavailable phosphorus (S-BioP), and (**E**) soluble reactive phosphorus (SRP), with turbidity in formazin nephelometric units (FNU). Dark grey circles with a solid blue line are for 2020; light green circles with a dashed blue line are for 2022; and light blue circles with a dotted blue line are for 2023. Boxplots for each of the study periods showing the results for (**B**) TP, (**D**) S-BioP, and (**F**) SRP

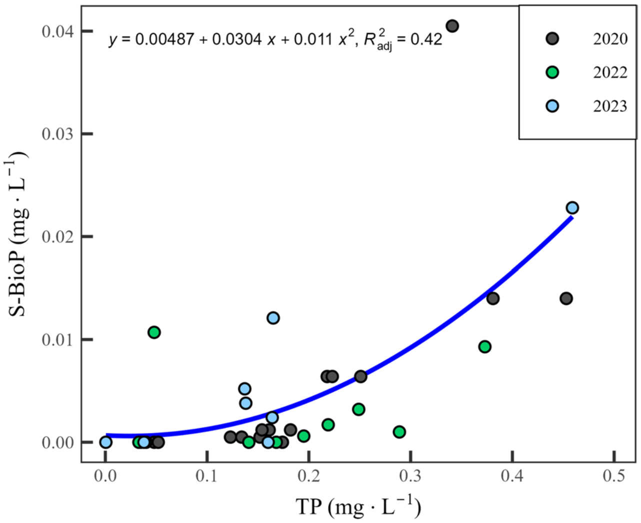

Fig. 6 Second order polynomial fitted to sediment-bound bioavailable phosphorus (S-BioP) plotted against total phosphorus (TP)

al. 2007) and significant loading of black carbon (i.e. charcoal; Wagner et al. 2015). Fine-grained sediment can travel long distances and may cause accelerated rates of deposition in alluvial fans and floodplains. These sediments may also become trapped within the gravel-bed matrix of the stream and remain available for future mobilization (Petticrew et al. 2007; Harper et al. 2017). Eder et al. (2014) conducted two flushing experiments on a small stream, during which they reported an increase in the sediment load of a downstream reach due to sediment resuspension.

Wildfire sediments were likely transported to the channel and riparian areas during WY 2022 and flushed in 2023 as a result of climatic variability. Data from the Pickfoot SNOTEL site indicate that precipitation first fell over the burn area on October 11, 2021, likely as snow. The historically low snowpack and subsequent below normal streamflow during water year 2022 would have limited sediment transport capacity to effectively flush sediments from the channel. Instead, it is likely that storm activity during July and August of 2022 redistributed wildfire sediments from the hillslope to the channel. A near normal snowpack and above average streamflow in 2023 would then have provided greater transport capacity to flush sediments previously deposited in 2022.

Sediment in Camas Creek is primarily derived from proximal sources. Hysteresis analysis of the turbidity-streamflow relationship indicated Camas Creek was preferential towards positive hysteresis events, where the supply of sediment is exhausted or interrupted before peak streamflow. This pattern is often attributed to sediments sourced from nearby riparian areas or within the channel (Gao and Josefson 2012; Mukundan et al. 2013; Hamshaw et al. 2018; Jing et al. 2025). Snowmelt is also a major driver of this type of hysteresis pattern due to the higher channel concentrated flows (Iida et al. 2012; Zhang et al. 2023). Positive hysteresis may also indicate a degree of hillslope to channel disconnectivity (Keesstra et al. 2019; Malutta et al. 2020; Clark et al. 2025) where hillslope sediments propagate towards the watershed outlet in a lagged response relative to streamflow and precipitation.

If sediments are overwhelmingly derived from the channel and riparian areas of Camas Creek, this may help explain the observed phosphorus response lag. For example,

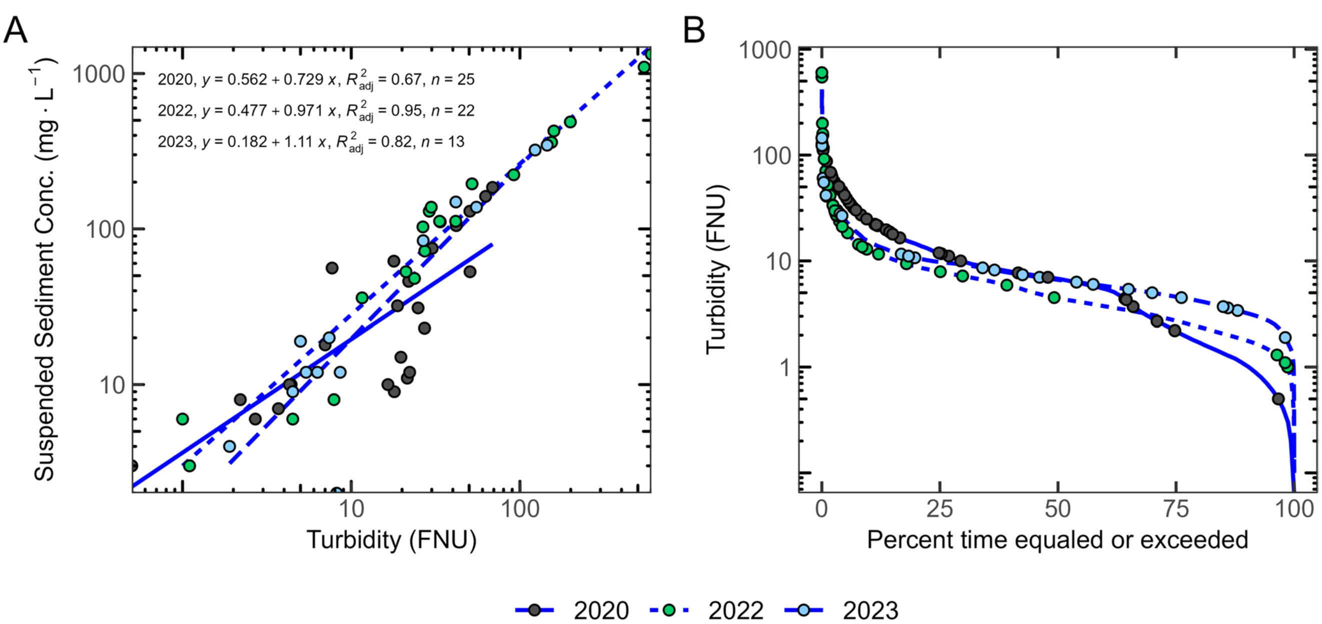

Fig. 7 (**A**) Suspended-sediment concentration and turbidity regression models and (**B**) turbidity concentration duration curves for each studied year. Points are discrete samples and turbidity is in formazin nephelometric units (FNU)

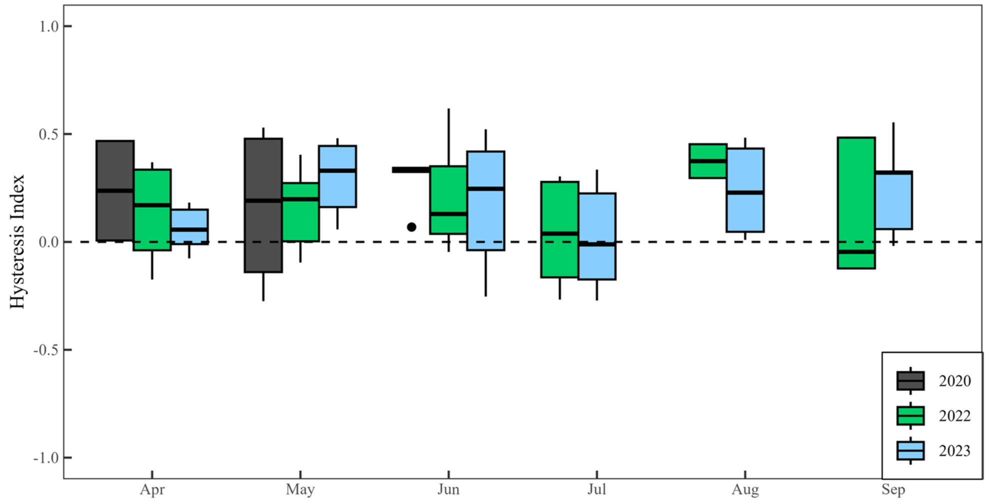

Fig. 8 Boxplots showing hysteresis indices grouped by month. No data were collected for July through August in the studied prefire year (2020)

sediments may have been delivered to the channel during snowmelt and summer precipitation events in 2022. Then, during 2023, those sediments were flushed from the channel during flooding that occurred during spring snowmelt. It is also possible that the phosphorus bound to sediments delivered to the channel after the first snowmelt season actively desorbed during the late summer when pH and DO fluctuate dramatically throughout the day. The phosphorus retention capacity of riverbed sediments decreases as pH increases due to the competition between hydroxyl ions and phosphorus ions (House 2003).

5 Conclusions

Our results suggest that postfire climate and catchment morphology play a role in attenuating water quality response to wildfire. The move from site USGS 06076600, which was near the mouth of Camas Creek and was sampled before the fire, to a new site 4.3 km upstream (USGS 06076590) after the fire did not affect our findings, therefore postfire changes observed (or not observed) can reasonably be attributed to fire effects. In our study, fire did not significantly alter the turbidity versus TP relationship nor the turbidity versus S-BioP relationship. Similarly, the TP versus S-BioP relationship was not significantly altered by the fire. The turbidity versus SRP relationship did change significantly. In postfire year 2023, there is much more SRP per unit TP than was observed in postfire year 2022. This suggests a lagged response in SRP potentially influenced by sediment retention in the channel. Though there was no observable increase in S-BioP, an increase in SRP may consequently contribute to excessive algal growth in the Smith River at timescales not captured in this study.

Results from this study also demonstrate the benefits of combining discrete water quality samples with high-frequency turbidity sensors to characterize postfire sediment and phosphorus dynamics. As is often the case within a given watershed, the SSC versus turbidity relationship is very strong (Grayson et al. 1996; Davies-Colley and Smith 2001). In-stream turbidity sensors detected increases to ambient turbidity in Camas Creek after the 2021 wildfire with the greatest difference being between prefire and 2-years postfire. These sensors also allowed for the examination and interpretation of concentration-streamflow hysteresis at the event scale through which we determined sediments in Camas Creek are primarily derived from channel and riparian areas. This finding indicates a slight hillslope to channel sediment dis-connectivity that may have influenced our postfire P observations.

Within the next century, over one-third of western watersheds are expected to have greater than 100% increase in sedimentation rate due to wildfires (Sankey et al. 2017). As drought and fire occurrence continue to affect western water supplies, understanding the dynamic and variable response in sediment and nutrient loading after wildfire can be used to better predict the long-term effects to water quality. As such, findings from this study may provide local agencies with strategies to aid in accounting for hydrologic extremes and disturbances (i.e., wildfire) in potential pollutant load allocations for an affected waterbody.

Acknowledgements The authors wish to gratefully thank Montana Department of Environmental Quality, and the U.S. Geological Survey Water Resources Mission Area for providing the resources and data collection necessary to complete the study. We also thank Natalie Schmer, Theodore Barnhart, and one anonymous reviewer for peer reviews. Any use of trade, firm, or product names is for descriptive purposes only and does not imply endorsement by the U.S. Government.

Data availability The data used in support of the findings of this work are available from the U.S. Geological Survey National Water Information System (U.S. Geological Survey [2025]; https://doi.org/10.5066/F7P55KJN), the National Water Quality Monitoring Council

(2025; https://doi.org/10.5066/P9QRKUVJ), and the U.S. Department of Agriculture, Natural Resource Conservation Service Water and Climate Information System (U.S. Department of Agriculture [2025]; https://nwcc-apps.sc.egov.usda.gov/).

Declarations

Conflict of interest The authors declare no conflicts of interest.

References

Bell C, Suplee M, Kron D, Metzner G, Regensburger E, Meredith C, Weir S (2024) 2018–2020 Smith River Algae Study. https://deq.mt.gov/files/Water/WQPB/Reports/2018-2020_Smith_River_Algae_Study_OCT2024_FINAL.pdf

Bladon KD, Emelko MB, Silins U, Stone M (2014) Wildfire and the future of water supply. Environ Sci Technol 48:8936–8943. https://doi.org/10.1021/es500130g

Bodí MB, Martin DA, Balfour VN et al (2014) Wildland fire ash: production, composition and eco-hydro-geomorphic effects. Earth-Sci Rev 130:103–127. https://doi.org/10.1016/j.earscirev.2013.12.007

Bright CE, Mager SM (2020) A national-scale study of spatial variability in the relationship between turbidity and suspended sediment concentration and sediment properties. River Res Appl 36:1449–1459. https://doi.org/10.1002/rra.3679

Burkle LA, Myers JA, Belote RT (2015) Wildfire disturbance and productivity as drivers of plant species diversity across spatial scales. Ecosphere 6:1–14. https://doi.org/10.1890/ES15-00438.1

Burn Severity Portal, Provisional Initial Assessments (2021) 2021 Montana: WOODS CREEK mt4655111135620210710. Accessed [January, 17, 2024] from https://burnseverity.cr.usgs.gov/products/provisionalIA

Busby DM, Wilcox AC (2024) Hydrogeomorphic response of steep streams following severe wildfire in the Western Cascades, Oregon. Earth Surf Process Landf 49:4570–4586. https://doi.org/10.1002/esp.5982

Clark GD, Murphy SF, Skalak K et al (2025) Hysteretic response of suspended-sediment in wildfire affected watersheds of the Pacific Northwest and Southern Rocky Mountains. Earth Surf Process Landforms. https://doi.org/10.1002/esp.6067

R Core Team (2024) R: A Language and Environment for Statistical Computing. Version 4.5.2. R Foundation for Statistical Computing, Vienna, Austria. <https://www.R-project.org/

Davies-Colley RJ, Smith DG (2001) Turbidity, suspended sediment, and water clarity: A review. J Am Water Resour Assoc 37. https://doi.org/10.1111/j.1752-1688.2001.tb03624.x

Dodds WK (1991) Factors associated with dominance of the filamentous green alga cladophora glomerata. Water Res 25:1325–1332. https://doi.org/10.1016/0043-1354(91)90110-C

Dodds WK, Smith VH, Zander B (1997) Developing nutrient targets to control benthic chlorophyll levels in streams: a case study of the Clark Fork River. Water Res. https://doi.org/10.1016/S0043-1354(96)00389-2

Eder A, Exner-Kittridge M, Strauss P, Blöschl G (2014) Re-suspension of bed sediment in a small stream – results from two flushing experiments. Hydrol Earth Syst Sci 18:1043–1052. https://doi.org/10.5194/hess-18-1043-2014

Emelko MB, Stone M, Silins U et al (2016) Sediment-phosphorus dynamics can shift aquatic ecology and cause downstream legacy effects after wildfire in large river systems. Glob Chang Biol 22:1168–1184. https://doi.org/10.1111/gcb.13073

Follmi D, Baartman J, Benali A, Nunes JP (2022) How do large wildfires impact sediment redistribution over multiple decades? Earth Surf Process Landf 47:3033–3050. https://doi.org/10.1002/esp.5441

Freistadt C, Maas C, Tran M et al (2024) Smith River State Park: Visitor Use and Monitoring Report 2024. Helena, MT. https://fwp.mt.gov/binaries/content/assets/fwp/stateparks/smith-river/management/smith-river-annual-report---2024.pdf

Froelich PN (1988) Kinetic control of dissolved phosphate in natural rivers and estuaries: a primer on the phosphate buffer mechanism. Limnol Oceanogr. https://doi.org/10.4319/lo.1988.33.4part2.0649

Gao P, Josefson M (2012) Event-based suspended sediment dynamics in a central New York watershed. Geomorphology. https://doi.org/10.1016/j.geomorph.2011.11.007

Geological Survey US (2024) Annual NLCD collection 1 science products (ver. 1.1, June 2025). U S Geol Surv Data Release. https://doi.org/10.5066/P94UXNTS. accessed [October 27, 2024]

Gray JR, Glysson GD, Turcios LM, Schwarz GE (2000) Comparability of Suspended-Sediment Concentration and Total Suspended Solids Data. US Geological Survey Water Resource Investigations Report 00-4191. https://water.usgs.gov/osw/pubs/WRIR00-4191.pdf

Grayson RB, Finlayson BL, Gippel CJ, Hart BT (1996) The potential of field turbidity measurements for the computation of total phosphorus and suspended solids loads. J Environ Manage 47:257–267. https://doi.org/10.1006/jema.1996.0051

Guy HP (1969) Laboratory theory and methods for sediment analysis. Techniques of Water-Resources Investigations of the United States Geological Survey Laboratory: book 5. https://pubs.usgs.gov/twri/twri5c1/

Hamshaw SD, Dewoolkar MM, Schroth AW et al (2018) A new machine-learning approach for classifying hysteresis in suspended-sediment discharge relationships using high-frequency monitoring data. Water Resour Res. https://doi.org/10.1029/2017WR022238

Hanna M (1989) Biologically available phosphorus: estimation and prediction using an anion-exchange resin. Can J Fish Aquat Sci 46:638–643. https://doi.org/10.1139/f89-081

Harper SE, Foster IDL, Lawler DM et al (2017) The complexities of measuring fine sediment accumulation within gravel-bed rivers. River Res Appl 33:1575–1584. https://doi.org/10.1002/rra.3198

Hauer F, Spencer C (1998) Phosphorus and nitrogen dynamics in streams associated with wildfire: a study of immediate and long-term effects. Int J Wildland Fire 8:183. https://doi.org/10.1071/WF9980183

Hohner AK, Rhoades CC, Wilkerson P, Rosario-Ortiz FL (2019) Wildfires alter forest watersheds and threaten drinking water quality. Acc Chem Res. https://doi.org/10.1021/acs.accounts.8b00670

House WA (2003) Geochemical cycling of phosphorus in rivers. Appl Geochem 18:739–748. https://doi.org/10.1016/S0883-2927(02)00158-0

Iida T, Kajihara A, Okubo H, Okajima K (2012) Effect of seasonal snow cover on suspended sediment runoff in a mountainous

catchment. J Hydrol 428–429. https://doi.org/10.1016/j.jhydrol.2012.01.029
Jakus PM, Nelson N, Ostermiller J (2017) Using survey data to determine a numeric criterion for nutrient pollution. Water Resour Res 53:10188–10200. https://doi.org/10.1002/2017WR021527
Jing T, Zeng Y, Fang N et al (2025) A review of suspended sediment hysteresis. Water Resour Res. https://doi.org/10.1029/2024WR037216
Jumps N, Gray AB, Guilinger JJ, Cowger WC (2022) Wildfire impacts on the persistent suspended sediment dynamics of the Ventura River, California. J Hydrol Reg Stud 41:101096. https://doi.org/10.1016/j.ejrh.2022.101096
Keesstra SD, Davis J, Masselink RH et al (2019) Coupling hysteresis analysis with sediment and hydrological connectivity in three agricultural catchments in Navarre, Spain. J Soils Sediments 19:1598–1612. https://doi.org/10.1007/s11368-018-02223-0
Koontz MJ, North MP, Werner CM et al (2020) Local forest structure variability increases resilience to wildfire in dry western U.S. coniferous forests. Ecol Lett 23:483–494. https://doi.org/10.1111/ele.13447
Lane PNJ, Sheridan GJ, Noske PJ, Sherwin CB (2008) Phosphorus and nitrogen exports from SE Australian forests following wildfire. J Hydrol 361:186–198. https://doi.org/10.1016/j.jhydrol.2008.07.041
Lloyd CEM, Freer JE, Johnes PJ, Collins AL (2016) Technical note: testing an improved index for analysing storm discharge-concentration hysteresis. Hydrol Earth Syst Sci. https://doi.org/10.5194/hess-20-625-2016
Malmon DV, Reneau SL, Katzman D et al (2007) Suspended sediment transport in an ephemeral stream following wildfire. J Geophys Res Earth Surf. https://doi.org/10.1029/2005JF000459
Malutta S, Kobiyama M, Chaffe PLB, Bonumá NB (2020) Hysteresis analysis to quantify and qualify the sediment dynamics: state of the art. Water Sci Technol. https://doi.org/10.2166/wst.2020.279
Mataix-Solera J, Cerdà A, Arcenegui V et al (2011) Fire effects on soil aggregation: a review. Earth Sci Rev 109:44–60. https://doi.org/10.1016/j.earscirev.2011.08.002
McDowell RW, Sharpley AN (2003) Uptake and release of phosphorus from overland flow in a stream environment. J Environ Qual 32:937–948. https://doi.org/10.2134/jeq2003.9370
McGuire LA, Ebel BA, Rengers FK et al (2024) Fire effects on geomorphic processes. Nat Rev Earth Environ 5:486–503. https://doi.org/10.1038/s43017-024-00557-7
Monitoring Trends in Burn Severity (2022) MTBS Project Homepage, USDA Forest Service/U.S. Geological Survey, accessed [November 16, 2024], at https://www.mtbs.gov
Mukundan R, Pierson DC, Schneiderman EM et al (2013) Factors affecting storm event turbidity in a New York City water supply stream. Catena. https://doi.org/10.1016/j.catena.2013.02.002
Murphy BP, Czuba JA, Belmont P (2019) Post-wildfire sediment cascades: a modeling framework linking debris flow generation and network-scale sediment routing. Earth Surf Process Landforms. https://doi.org/10.1002/esp.4635
National Water Quality Monitoring Council; U.S. Geological Survey; U.S. Environmental Protection Agency (2025) Water Quality Portal. Accessed [November 16, 2024]. https://doi.org/10.5066/P9QRKUVJ
Natural Resources Conservation Service (2024) U.S. Department of Agriculture. National Water and Climate Center Public Reports Accessed [November 3, 2024] from https://wcc.sc.egov.usda.gov/nwcc/site?sitenum=690
Natural Resources Conservation Service (2025) U.S. Department of Agriculture Web Soil Survey. Accessed [April 18, 2025] from https://websoilsurvey.nrcs.usda.gov/
Neary DG, Ryan KC, DeBano LF (2005) Wildland fire in ecosystems: effects of fire on soils and water. Gen. Tech. Rep. RMRS-GTR-42-vol.4. Ogden. U.S. Department of Agriculture, Forest Service, UT. https://doi.org/10.2737/RMRS-GTR-42-V4. Rocky Mountain Research Station
Neely AB, Moon S, DiBiase RA et al (2024) The grain size of sediments delivered to steep debris-flow prone channels prior to and following wildfire. Earth Surf Process Landforms 49:2110–2133. https://doi.org/10.1002/esp.5819
Nimick DA, Gammons CH, Parker SR (2011) Diel biogeochemical processes and their effect on the aqueous chemistry of streams: a review. Chem Geol 283:3–17. https://doi.org/10.1016/j.chemgeo.2010.08.017
Owens PN, Batalla RJ, Collins AJ et al (2005) Fine-grained sediment in river systems: environmental significance and management issues. River Res Appl 21:693–717. https://doi.org/10.1002/rra.878
Petticrew EL, Krein A, Walling DE (2007) Evaluating fine sediment mobilization and storage in a gravel-bed river using controlled reservoir releases. Hydrol Process 21:198–210. https://doi.org/10.1002/hyp.6183
Ranalli A (2004) A summary of the scientific literature on the effects of fire on the concentration of nutrients in surface waters. https://doi.org/10.3133/ofr20041296. US Geological Survey Open-File Report 2004 – 1296
Records RM, Wohl E, Arabi M (2016) Phosphorus in the river corridor. Earth Sci Rev 158:65–88. https://doi.org/10.1016/j.earscirev.2016.04.010
Rengers FK, McGuire LA, Kean JW et al (2021) Movement of sediment through a burned landscape: sediment volume observations and model comparisons in the San Gabriel Mountains, California, USA. J Geophys Res Earth Surf. https://doi.org/10.1029/2020JF006053
Reynolds M, Brandt T (2005) Geologic map of the Canyon ferry dam 30’ x 60’ quadrangle, west-central Montana. US Geological Survey Scientific Investigations Map 2860. https://pubs.usgs.gov/sim/2005/2860/
Riley KL, Grenfell IC, Finney MA, Shaw JD (2021) TreeMap 2016: a tree-level model of the forests of the conterminous United States circa 2016. Forest Service Research Data Archive. https://doi.org/10.2737/RDS-2021-0074
Robinne F, Hallema DW, Bladon KD et al (2021) Scientists’ warning on extreme wildfire risks to water supply. Hydrol Process. https://doi.org/10.1002/hyp.14086
Rust AJ, Hogue TS, Saxe S, McCray J (2018) Post-fire water-quality response in the western United States. Int J Wildland Fire. https://doi.org/10.1071/WF17115
Ryan SE, Dwire KA, Dixon MK (2011) Impacts of wildfire on runoff and sediment loads at Little Granite Creek, western Wyoming. Geomorphology. https://doi.org/10.1016/j.geomorph.2011.01.017
Sankey JB, Kreitler J, Hawbaker TJ et al (2017) Climate, wildfire, and erosion ensemble foretells more sediment in western USA watersheds. Geophys Res Lett. https://doi.org/10.1002/2017GL073979
Schaller J, Tischer A, Struyf E et al (2015) Fire enhances phosphorus availability in topsoils depending on binding properties. Ecology 96:1598–1606. https://doi.org/10.1890/14-1311.1
Searle SR, Speed FM, Milliken GA (1980) Population marginal means in the linear model: an alternative to least squares means. Am Stat. https://doi.org/10.1080/00031305.1980.10483031
Shakesby R, Doerr S (2006) Wildfire as a hydrological and geomorphological agent. Earth Sci Rev 74:269–307. https://doi.org/10.1016/j.earscirev.2005.10.006
Smith HG, Sheridan GJ, Lane PNJ et al (2011) Wildfire effects on water quality in forest catchments: a review with implications for water supply. J Hydrol 396:170–192. https://doi.org/10.1016/j.jhydrol.2010.10.043

Souza-Alonso P, Prats SA, Merino A et al (2024) Fire enhances changes in phosphorus (P) dynamics determining potential post-fire soil recovery in Mediterranean woodlands. Sci Rep 14:21718. https://doi.org/10.1038/s41598-024-72361-8

Standard M (2017) 2540 Solids. In Standard Methods For the Examination of Water and Wastewater. American Public Health Association. https://doi.org/10.2105/SMWW.2882.030

Stevenson RJ, Bennett BJ, Jordan DN, French RD (2012) Phosphorus regulates stream injury by filamentous green algae, DO, and pH with thresholds in responses. Hydrobiologia 695:25–42. https://doi.org/10.1007/s10750-012-1118-9

Stone M, Krishnappan BG, Silins U et al (2021) A new framework for modelling fine sediment transport in rivers includes flocculation to inform reservoir management in wildfire impacted watersheds. Water 13:2319. https://doi.org/10.3390/w13172319

Strand EK, Satterberg KL, Hudak AT et al (2019) Does burn severity affect plant community diversity and composition in mixed conifer forests of the United States Intermountain West one decade post fire? Fire Ecol 15:25. https://doi.org/10.1186/s42408-019-0038-8

Suplee MW (2021) Determination of bioavailable phosphorus from water samples with low suspended sediment using an anion exchange resin method. MethodsX 8:101343. https://doi.org/10.1016/j.mex.2021.101343

Suplee MW, Watson V, Teply M, McKee H (2009) How green is too green? Public opinion of what constitutes undesirable algae levels in streams. J Am Water Resour Assoc 45:123–140. https://doi.org/10.1111/j.1752-1688.2008.00265.x

Temporetti P, Beamud G, Nichela D et al (2019) The effect of pH on phosphorus sorbed from sediments in a river with a natural pH gradient. Chemosphere 228:287–299. https://doi.org/10.1016/j.chemosphere.2019.04.134

Turnipseed DP, Sauer VB (2010) Discharge measurements at gaging stations. US Geological Survey Techniques and Methods 3-A8. https://doi.org/10.3133/tm3A8

US Geological Survey (2025) National Water Information System data available on the World Wide Web (USGS Water Data for the Nation), accessed [November 16, 2024], at http://waterdata.usgs.gov/nwis/. https://doi.org/10.5066/F7P55KJN

US Department of Agriculture, Natural Resource Conservation Service, National Water and Climate Center (2025) Air and Water Database. Water and Climate Information System. Accessed [February 22, 2024], at https://nwcc-apps.sc.egov.usda.gov/

US Geological Survey (2019) The StreamStats Program. https://streamstats.usgs.gov/ss/, accessed on April 18, 2025

Uusitalo R, Ekholm P (2003) Phosphorus in runoff assessed by anion exchange resin extraction and an algal assay. J Environ Qual 32:633–641. https://doi.org/10.2134/jeq2003.6330

Uusitalo R, Yli-Halla M, Turtola E (2000) Suspended soil as a source of potentially bioavailable phosphorus in surface runoff waters from clay soils. Water Res 34. https://doi.org/10.1016/S0043-1354(99)00419-4

Vadeboncoeur Y, Moore MV, Stewart SD et al (2021) Blue waters, green bottoms: benthic filamentous algal blooms are an emerging threat to clear lakes worldwide. Bioscience 71:1011–1027. https://doi.org/10.1093/biosci/biab049

Wagner R, Mattraw H, Ritz G, Smith B (2006) Guidelines and Standard Procedures for Continuous Water-Quality Monitors: Site Selection, Field Operation, Calibration, Record Computation, and Reporting. US Geological Survey Techniques and Methods 1-D3. https://pubs.usgs.gov/tm/2006/tm1D3/

Wagner S, Cawley KM, Rosario-Ortiz FL, Jaffé R (2015) In-stream sources and links between particulate and dissolved black carbon following a wildfire. Biogeochemistry 124:145–161. https://doi.org/10.1007/s10533-015-0088-1

Watt C, Emelko MB, Silins U et al (2021) Anthropogenic and climate-exacerbated landscape disturbances converge to alter phosphorus bioavailability in an oligotrophic river. Water 13:3151. https://doi.org/10.3390/w13223151

Wester T, Wasklewicz T, Staley D (2014) Functional and structural connectivity within a recently burned drainage basin. Geomorphology 206:362–373. https://doi.org/10.1016/j.geomorph.2013.10.011

Wilkes MA, Gittins JR, Mathers KL et al (2019) Physical and biological controls on fine sediment transport and storage in rivers. WIREs Water. https://doi.org/10.1002/wat2.1331

Williams CJ, Pierson FB, Robichaud PR et al (2016) Structural and functional connectivity as a driver of hillslope erosion following disturbance. Int J Wildland Fire 25:306–321. https://doi.org/10.1071/WF14114

Withers PJA, Jarvie HP (2008) Delivery and cycling of phosphorus in rivers: a review. Sci Total Environ 400:379–395. https://doi.org/10.1016/j.scitotenv.2008.08.002

Withers P, Neal C, Jarvie H, Doody D (2014) Agriculture and eutrophication: where do we go from here? Sustainability 6:5853–5875. https://doi.org/10.3390/su6095853

Wurtsbaugh WA, Paerl HW, Dodds WK (2019) Nutrients, eutrophication and harmful algal blooms along the freshwater to marine continuum. WIREs Water. https://doi.org/10.1002/wat2.1373

Yu M, Bishop TFA, van Ogtrop FF (2019) Assessment of the decadal impact of wildfire on water quality in forested catchments. Water 11:533. https://doi.org/10.3390/w11030533

Zhang T, Li D, East AE et al (2023) Shifted sediment-transport regimes by climate change and amplified hydrological variability in cryosphere-fed rivers. Sci Adv. https://doi.org/10.1126/sciadv.adi5019

Zhou J, Leavitt PR, Zhang Y, Qin B (2022) Anthropogenic eutrophication of shallow lakes: is it occasional? Water Res 221:118728. https://doi.org/10.1016/j.watres.2022.118728

Publisher's note Springer Nature remains neutral with regard to jurisdictional claims in published maps and institutional affiliations.